J. Phys.: Condens. Matter **11** (1999) 1711–1722. Printed in the UK PII: S0953-8984(99)97009-1

The origin of the change in type of the majority carrier in $LaCo_{1-x}Ti_xO_3$ ($0.05 \leqslant x \leqslant 0.15$)

H Nakatsugawa and E Iguchi

Materials Science, Department of Mechanical Engineering and Materials Science, Faculty of Engineering, Yokohama National University, Tokiwadai, Hodogaya-Ku, Yokohama 240-8501, Japan

Received 27 August 1998, in final form 13 November 1998

Abstract. Electrical transport properties of polycrystalline ceramic specimens of the system $LaCo_{1-x}Ti_xO_3$ ($x = 0.05$, 0.10, and 0.15) have been investigated as functions of temperature by means of complex-plane impedance analysis, dielectric properties, four-probe dc conductivity, Seebeck coefficients, and magnetic susceptibilities. The type of the majority carrier changes from electrons to holes when x increases from 0.10 to 0.15, because the Seebeck coefficient changes from negative to positive with x increasing from 0.10 to 0.15. The complex-plane impedance analysis distinguishes the bulk conduction from the conduction across grain boundaries. In a specimen with $x = 0.15$, the activation energy in the bulk conduction is nearly equal to that for the dielectric relaxation. This implies that the hopping process of small polarons of holes dominates the transport properties in this specimen above 190 K. The temperature dependencies of the magnetic susceptibilities indicate that the number of high-spin Co^{3+} ions ($S = 2$) decreases with increasing x. The expansion of the lattice parameters and the increment of the c_H/a_H ratio with increasing x suggest that Ti^{4+} ions are preferentially substituted for low-spin Co^{III}, which relaxes the rhombohedral structural distortion in the $LaCo_{1-x}Ti_xO_3$ system. The change in the type of the charge carrier has been discussed in terms of the electronic structures deduced from these experimental results.

1. Introduction

Perovskite $LaCoO_3$ exhibits very interesting physical features such as magnetic properties due to the spin-state transition, the structural transition, the insulator–metal transition, and valence band states which have been investigated extensively [1–16]. The spin-state transition indicates that $LaCoO_3$ involves various spin states of Co ions, the relative ratios of which depend on temperature [4, 16]. The relative stability of these spin states has been studied from the theoretical point of view [17–20]. In order to investigate the electronic structures, the electrical transport properties have been elucidated, because the spin state of the Co ions governs the nature of the carrier [16, 21]. Referring to polaron theory [22–24], our previous study has shown that the dominant conduction in $LaCoO_3$ at $T > 120$ K is due to a hopping process of small polarons of holes which are created by electron excitation through the band gap of 0.2 eV [21]. Hole-doped $La_{1-x}Sr_xCoO_3$ exhibits similar polaronic conduction as well [25].

Electron doping in $LaCoO_3$ by substitution of Ti for Co must induce remarkable changes in transport properties and electronic structures, i.e., spin states. $LaCoO_3$ is a monovalent system but $LaCo_{1-x}Ti_xO_3$ is a mixed-valence system, because the charge neutrality requires divalent Co ions. Thus, $LaCo_{1-x}Ti_xO_3$ is expected to be a mixture of LS Co^{III} (t_{2g}^6), LS Co^{II} ($t_{2g}^6e_g^1$), HS Co^{3+} ($t_{2g}^4e_g^2$), and HS Co^{2+} ($t_{2g}^5e_g^2$), the relative ratios of these spin-state Co ions being

0953-8984/99/071711+12$19.50

dependent on both x and T, where LS and HS are abbreviations for low- and high-spin states. It is noteworthy that the type of the majority carrier changes with increasing x in $LaCo_{1-x}Ti_xO_3$, because the Seebeck coefficient in the temperature range 300 K to 450 K is negative for $x = 0.05$ but positive at $T > 300$ K for $x = 0.15$ [26]. This change is probably caused by the alternation of the electronic structure due to the spin-state transition. Usually, electron doping enhances n-type semiconductivity, but this is not realized in this system. The relationship between the change in the type of the majority carrier and the spin-state transition is the main subject of the present study, which requires thus both transport and magnetic measurements as functions of temperature. Although Bahadur and Parkash carried out such measurements on this system above room temperature [26], experiments below room temperature are essential.

In view of the conduction due to the hopping processes of small polarons in $LaCoO_3$ and $La_{1-x}Sr_xCoO_3$ [21, 25], one expects similar conduction in $LaCo_{1-x}Ti_xO_3$. Among the various experimental means that can be used to address the polaron dynamics, investigating dielectric properties provides particularly important knowledge, because a hopping process of small polarons has a high probability of involving a dielectric relaxation. Our previous reports [21, 25, 27–38] show that a dielectric relaxation study provides significant results, leading directly to an electrical characterization, particularly of localized carriers such as polarons, and also to a transport kinetics via the hopping carriers. In order to investigate the charge dynamics (and/or polaron dynamics), a high-quality single crystal is required, because grain boundaries in sintered specimens hinder the study of transport phenomena [21, 25]. Even if a polycrystalline ceramic specimen is employed, however, the complex-plane impedance analysis distinguishes the bulk conduction from the conduction across the grain boundary and the transport across the electrode–specimen interface, if they exist [39–42]. The combination of the complex-plane impedance analysis and the dielectric measurements could thus be one of the most reliable means for investigating electrical transport in polycrystalline $LaCo_{1-x}Ti_xO_3$.

In view of this, the present study carries out complex-plane impedance analyses and measurements of four-probe dc conductivity, Seebeck coefficients, dielectric properties, and magnetic susceptibilities for $LaCo_{1-x}Ti_xO_3$ ($x = 0.05$, 0.10, and 0.15) as functions of temperature up to 330 K, then discusses the possibility of electrical transport due to the hopping process of small polarons, and speculates on the origin of the change in the type of the majority carrier when x increases from 0.10 to 0.15.

2. Experimental details

Polycrystalline specimens of $LaCo_{1-x}Ti_xO_3$ ($x = 0.05$, 0.10, and 0.15) were prepared by the conventional solid-state synthesis technique. La_2O_3, Co_3O_4, and TiO_2 powders were used. La_2O_3 was first fired in air at 1273 K for 10 h on Al_2O_3 boats. Then the appropriate mixtures of these powders were calcined in air at 1373 K for 24 h. This heating process was performed in total three times. Then, the powders were pressed into pellets and finally fired at 1623 K for 48 h in air. The Cu Kα powder x-ray diffraction pattern indicates a single phase of a rhombohedrally distorted perovskite structure with hexagonal cell parameters $a_H = 5.449$ Å and $c_H = 13.114$ Å for $x = 0.05$, $a_H = 5.456$ Å and $c_H = 13.134$ Å for $x = 0.10$, and $a_H = 5.468$ Å and $c_H = 13.167$ Å for $x = 0.15$. These lattice parameters correspond well to the ones reported by Bahadur and Parkash [26]. It is noteworthy that both of the lattice parameters, a_H and c_H, enlarge as the number of Ti ions increases. Furthermore, the c_H/a_H ratio also increases from 2.406 to 2.408 with x increasing from 0.05 to 0.15. The densities of the specimens were about 80% of the theoretical values. Chemical analyses by redox titration [43] determined the oxygen contents of the specimens, i.e., $LaCo_{0.95}Ti_{0.05}O_{2.99}$,

$LaCo_{0.90}Ti_{0.10}O_{3.00}$, and $LaCo_{0.85}Ti_{0.15}O_{2.98}$, slightly oxygen deficient in every specimen‡. The experimental error of the oxygen content is within ±3%.

A Keithley 619 resistance bridge, an Advantest TR 6871 digital multimeter, and an Advantest R 6161 power supply were used for the dc conductivity measurements by four-probe method. Using an HP 4284A LCR meter with the frequency range 20 Hz to 1 MHz, the capacitance and conductance were obtained as functions of temperature by the four-terminal pair ac impedance measurement method. The measured values of the capacitance and conductance were corrected by calibrating the capacitance and resistance of the leads as zero. An In–Ga alloy in a 7:3 ratio was used for the electrode. Evaporated gold was also used for the electrode, but no significant difference was found in the experimental results.

In order to check the surface capacitance effect, capacitance measurements were carried out at 200 K over the frequency range 10 kHz to 1 MHz by changing the thickness of the specimen from 1.2 to 0.6 mm, and the dielectric constants were independent of the thickness. Thus, surface effects were not included in the dielectric properties obtained in the present experiment. Seebeck coefficients were measured using a home-made device at $T < 330$ K. A copper–constantan thermocouple, precalibrated at 4.2, 77, and 273 K, was used for the temperature measurements. The magnetic susceptibilities were measured by using a SQUID (Quantum Design, MPMS).

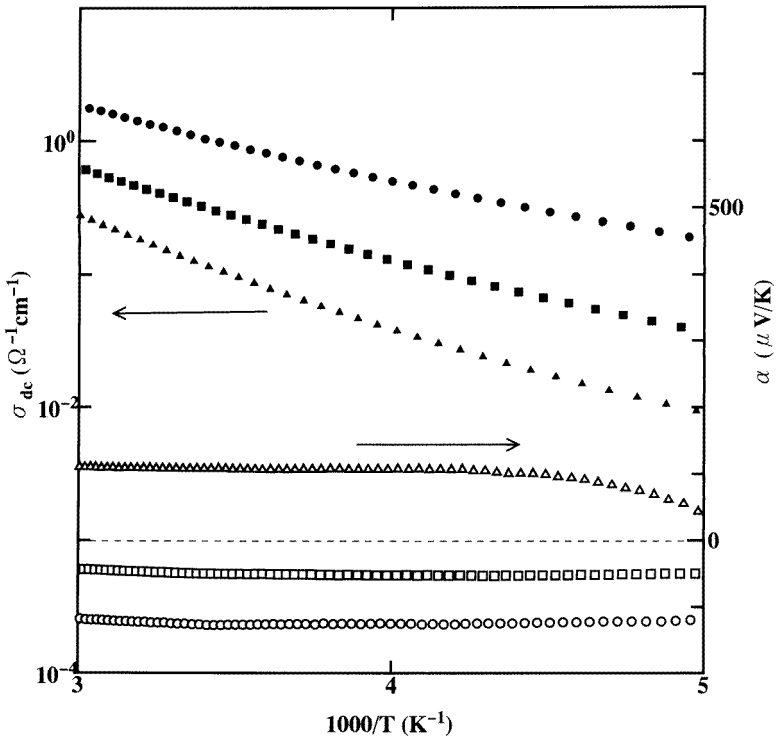

Figure 1. Arrhenius relations between σ_{dc} and $1/T$ for the $LaCo_{1-x}Ti_xO_3$ specimens with $x = 0.05$ (solid circles), $x = 0.10$ (solid squares), and $x = 0.15$ (solid triangles), where σ_{dc} is the dc conductivity obtained by the four-probe method. The temperature dependencies of the Seebeck coefficients (α) are also shown for $x = 0.05$ (open circles), $x = 0.10$ (open squares), and $x = 0.15$ (open triangles). The transverse broken line indicates $\alpha = 0$ μV K^{-1}.

‡ The chemical analysis was carried out at the Nissan Arc Company, Limited.

3. Results

Figure 1 shows the temperature dependence of the four-probe dc conductivity (σ_{dc}) for every specimen. The conductivity decreases with increasing x. The Seebeck coefficients (α) are also plotted in figure 1. The negative magnitudes for the Seebeck coefficients for the specimens with $x = 0.05$ and 0.10 indicate that electrons are the majority carriers, whereas holes are the majority carriers in the specimen with $x = 0.15$ at $T > 190$ K as indicated by the positive Seebeck coefficients. The Seebeck coefficient is for each specimen nearly independent of temperature for $T > 230$ K. Bahadur and Parkash reported a similar result for $x = 0.05$ and 0.15 for the temperature range 350 K to 450 K [26].

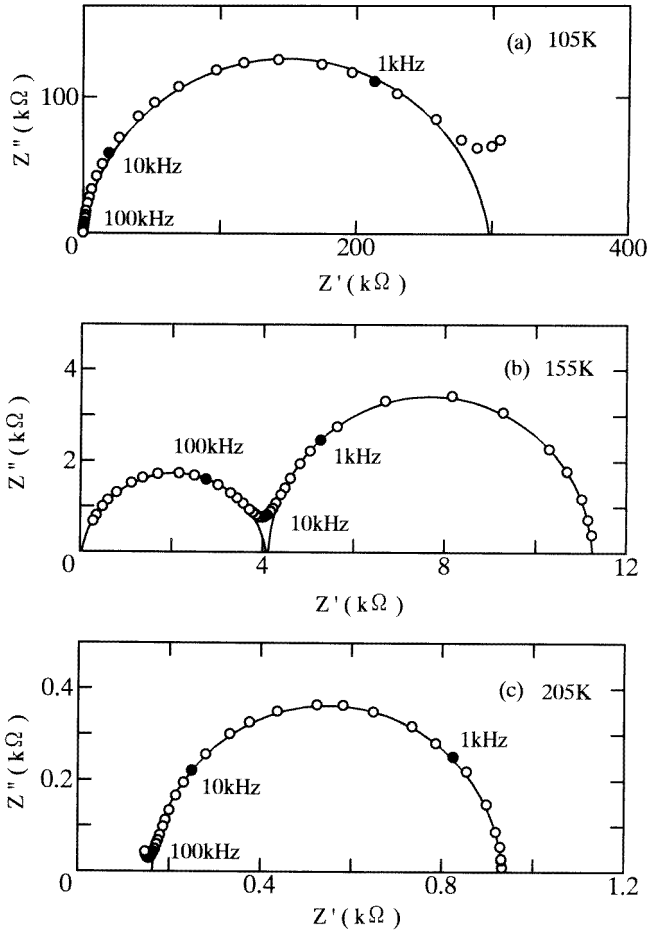

Figure 2. Complex-plane impedance analyses for the specimen with $x = 0.15$ at 105 K (a), 155 K (b), and 205 K (c), where Z' and Z'' represent the real and imaginary parts of the total impedance at each applied frequency. The highest resistance value of the highest-frequency arc is the resistance within the grains.

Following the theoretical procedures of the complex-plane impedance analysis [39–42], impedance plots at 105, 155, and 205 K for the specimen with $x = 0.15$ are shown in figure 2 in which the imaginary part of the total impedance (Z'') is plotted against the real part (Z') as a parametric function of frequency. The plots each contain a two-semicircular-arc structure, with

the highest-frequency arc crossing through the origin (the bulk conduction) and through the intermediate-frequency one (the conduction across the grain boundary). The full curves were obtained by least-mean-squares analyses. Since the lowest-frequency arc was not observed over the whole temperature region investigated here, there must be no electrode polarization in the interface barrier between the electrode and the specimen throughout the range of frequencies employed in the measurements. Theoretically, the highest resistance value of the intermediate arc is the total resistance in the grains and boundaries [39–42].

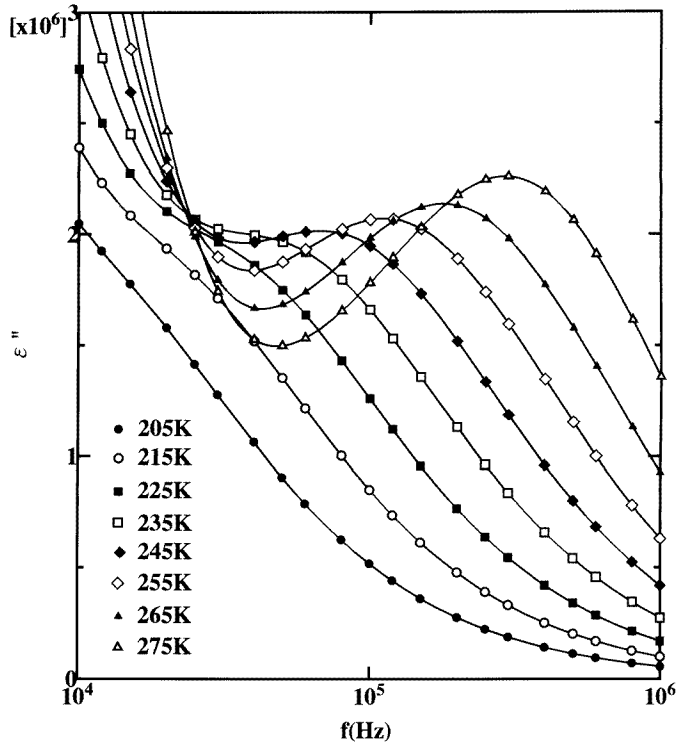

Figure 3. Frequency dependencies of the dielectric loss factor ε'' for 10 K increments in the range 205 K to 275 K for the specimen with $x = 0.15$.

Figure 3 displays the frequency dependencies of the dielectric loss factor (ε'') for the specimen with $x = 0.15$, for 10 K increments in the range 205 K to 275 K. In the specimens with $x = 0.05$ and 0.10, dielectric relaxation processes also occur at $T < 200$ K for the specimen with $x = 0.05$ and at $T < 230$ K for that with $x = 0.10$; these temperatures values are considerably lower than the resonance temperatures for the specimen with $x = 0.15$.

Employing the bulk conductivity (σ) determined from the highest resistance values of the highest-frequency arcs in the impedance analyses, figure 4 plots the Arrhenius relations of σT and $1/T$. At $T > 210$ K for $x = 0.05$, $T > 220$ K for $x = 0.10$, and $T > 190$ K for $x = 0.15$, each relation contains a linear portion with an activation energy of 0.21 eV for $x = 0.05$, 0.23 eV for $x = 0.10$, and 0.24 eV for $x = 0.15$. Like those for various oxides reported previously [21, 25, 27–38], the four-probe dc conductivities for these specimens overlap the conductivity estimated from the highest resistance values of the intermediate-frequency arcs, which are theoretically the total resistances in the grains and boundaries [39–42].

Figure 5 shows the temperature dependencies of the reciprocal molar magnetic

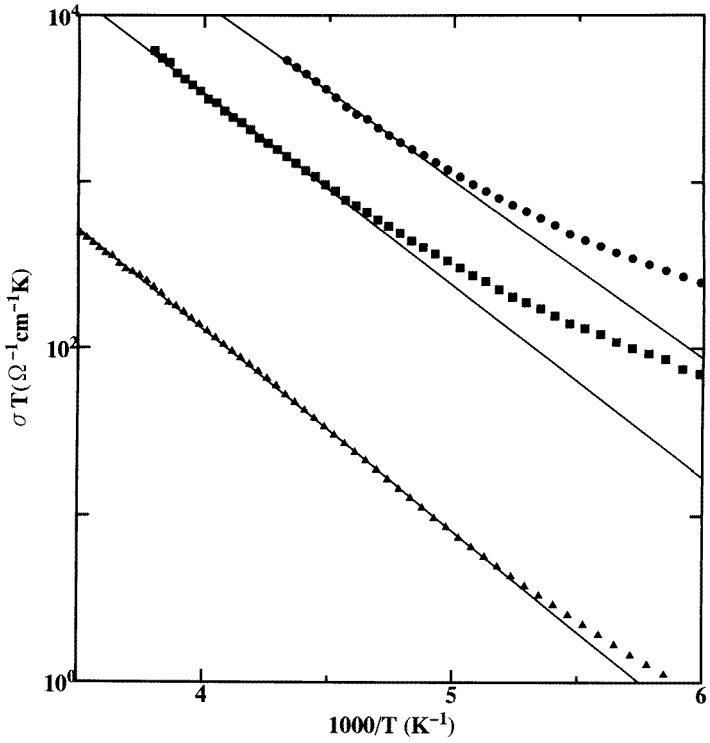

Figure 4. Arrhenius relations between σT and $1/T$ for the specimens with $x = 0.05$ (solid circles), $x = 0.10$ (solid squares), and $x = 0.15$ (solid triangles). The straight lines represent linear portions in the Arrhenius plots of the bulk conductivity.

susceptibilities (χ^{-1}) for these specimens. The susceptibilities were measured at temperatures in the range 10–330 K with the magnetic field of 1 T after the specimens had been cooled down in a field of 10 mT. The relation of χ^{-1} and T for each specimen contains a linear portion, at $T > 130$ K for $x = 0.05$, $T > 185$ K for $x = 0.10$, and $T > 205$ K for $x = 0.15$; this is indicative of the Curie–Weiss law with the formula $\chi = C/(T - \Theta)$, where C is the Curie constant and Θ is the Weiss temperature.

4. Discussion

4.1. Hopping conduction

The present study has succeeded in distinguishing the bulk conduction from the conduction across grain boundaries, using complex-plane impedance analyses. As described before, the linear relations in the Arrhenius plots of the bulk conductivity in figure 4 certainly favour adiabatic hopping conduction in the $LaCo_{1-x}Ti_xO_3$ system, because the polaron theory [22–24] predicts the following formula for such conduction:

$$\sigma T \propto \exp(-W_H/k_B T) \tag{1}$$

where W_H is the hopping energy of small polarons, and k_B is Boltzmann's constant, but the disordered energy is omitted because this is, in general, negligibly small in a crystalline lattice compared with W_H [44].

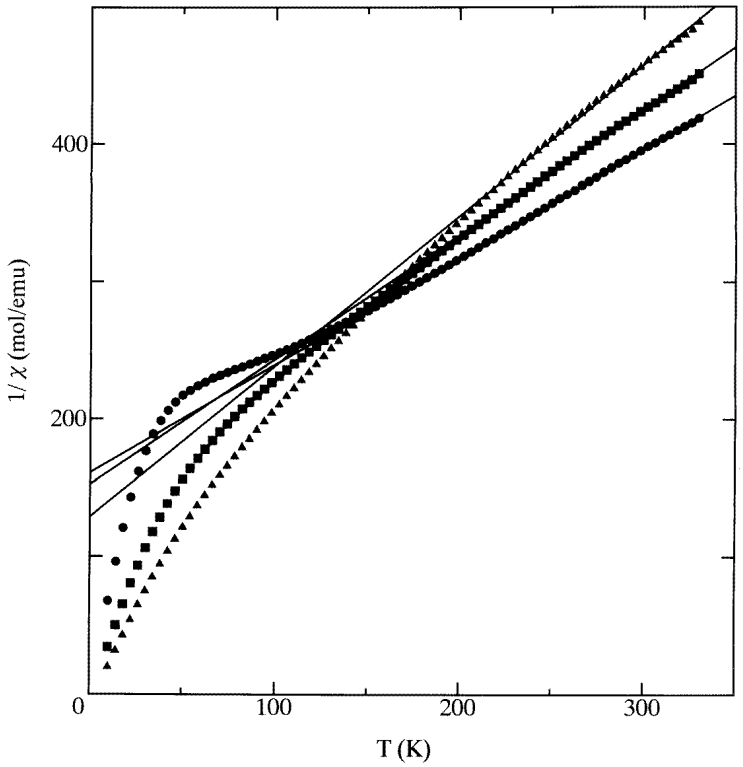

Figure 5. χ^{-1} versus T for the specimens with $x = 0.05$ (solid circles), $x = 0.10$ (solid squares), and $x = 0.15$ (solid triangles). The straight lines represent the Curie–Weiss laws with $\Theta = -205.9$ K, -168.1 K, and -117.5 K for the specimens with $x = 0.05$, 0.10, and 0.15, respectively.

The transport result in figure 4 certainly favours the polaronic scenario of bulk conduction. This is also evident from the dielectric properties, which are approximately described by Debye's theory, which formulates the dielectric loss factor as

$$\varepsilon'' = (\varepsilon_0 - \varepsilon_\infty)\frac{\omega\tau}{1 + (\omega\tau)^2} \tag{2}$$

where ε_0 and ε_∞ are the static and high-frequency dielectric constants, and ω is the applied angular frequency, i.e., $\omega = 2\pi f$ [45]. The relaxation time of the dielectric loss factor is given as $\tau = \tau_0 \exp(Q/k_B T)$, where Q is the activation energy required for the dielectric relaxation process and $1/\tau_0$ is the jump frequency. At a temperature T, the dielectric loss factor has its maximum at the resonance frequency $f_{\varepsilon''} = 1/2\pi\tau$. These relations yield the dielectric resonance condition as follows:

$$f_{\varepsilon''} \propto \exp(-Q/k_B T). \tag{3}$$

Figure 6 plots the Arrhenius relation of $f_{\varepsilon''}$ and $1/T$ for every specimen. A good straight line is obtained for the specimen with $x = 0.15$ at temperatures in the range 190 K to 280 K, and the least-mean-squares analysis yields $Q = 0.24$ eV which agrees very well with the activation energy required for the bulk conduction in figure 4. The majority carriers are holes in this specimen at $T > 200$ K because the Seebeck coefficients are positive. When a hopping process of small polarons is responsible for a dielectric relaxation, the activation energy, Q, is

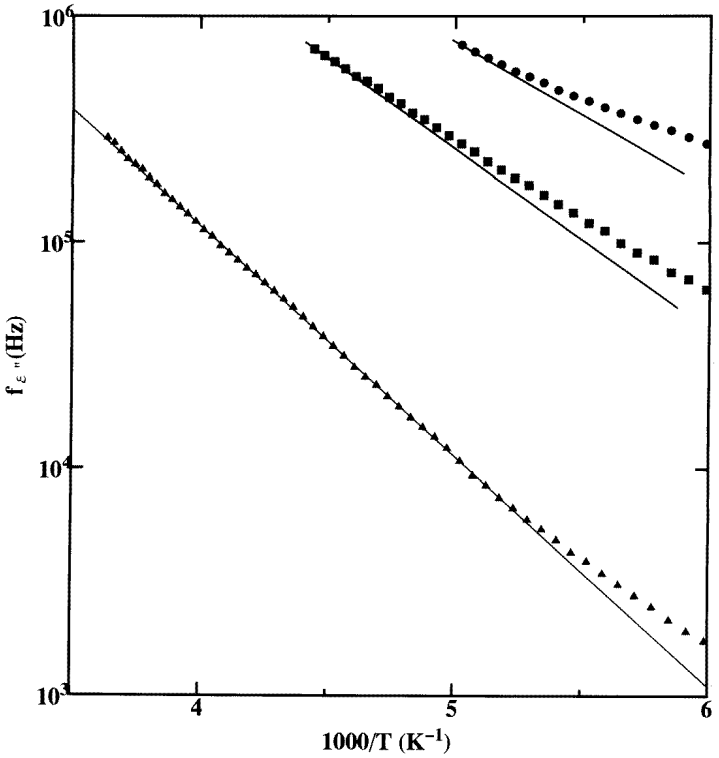

Figure 6. Arrhenius relations between $f_{\varepsilon''}$ and $1/T$ for the specimens with $x = 0.05$ (solid circles), $x = 0.10$ (solid squares), and $x = 0.15$ (solid triangles).

the hopping energy, i.e., $Q = W_H$ [21, 25, 27–38]. The agreement of the activation energies obtained independently leads to the conclusion that the hopping process of small polarons of holes dominates the electrical transport in the specimen with $x = 0.15$. It is very interesting that the hopping process of small polarons of holes also dominates the electrical conduction in $LaCoO_3$ at $T > 170$ K with the hopping energy $W_H = 0.25$ eV [21].

As shown in figure 4, the onset of a non-Arrhenius bulk conduction at low temperatures is found for each specimen. This is a general feature of small-polaron hopping [46, 47]. It arises as multiphonon jump processes are frozen out. The conduction at lower temperatures is then described by an extension of the Arrhenius small-polaron hopping into the non-Arrhenius regime. The temperature regions of the Arrhenius bulk conduction in the specimens with $x = 0.05$ and 0.10 are very narrow. This is because the impedance analyses for these specimens at higher temperatures require frequencies much higher than the maximum one in the present study, i.e., 1 MHz. In figure 6, there are also non-Arrhenius regimes for the specimens with $x = 0.05$ and 0.10 because the dielectric relaxation peaks appear at lower temperatures in the frequency range employed here. If frequencies much higher than 1 MHz were available, Arrhenius regimes at higher temperatures would appear. The non-Arrhenius regime of every specimen in figure 6 exhibits behaviour very similar to those in figure 4. Usually, Arrhenius relations of bulk conductivity like those shown in figure 4 have similar features to Arrhenius relations for dielectric resonances like those in figure 6, because the energies required in the two processes are nearly equal if conduction by small-polaron hopping is dominant [21, 36].

4.2. Spin states of Co ions

In the Curie–Weiss relation in the paramagnetic regime of figure 5, the magnitude of the Curie constant (C) decreases with increasing x, i.e., $C = 1.28$, 1.10, and 0.91 emu K mol^{-1} for $x = 0.05$, 0.10, and 0.15. This indicates that the relative ratio of Co^{3+} ($S = 2$) ions decreases with increasing x, because the effective magnetic moments ($\mu_{\rm eff} \simeq \sqrt{8C}\mu_{\rm B}$) are estimated to be $3.19\mu_{\rm B}$ for $x = 0.05$, $2.97\mu_{\rm B}$ for $x = 0.10$, and $2.70\mu_{\rm B}$ for $x = 0.15$, where $\mu_{\rm B}$ is the Bohr magneton. These experimental results are obtained at 130 K $< T <$ 330 K for $x = 0.05$, 185 K $< T <$ 330 K for $x = 0.10$, and 205 K $< T <$ 330 K for $x = 0.15$. In the temperature regions for which the magnetic moments are estimated, the hopping process of small polarons dominates the electrical conduction in each specimen as described before. Señarís-Rodríguez and Goodenough have reported that the parent system $LaCoO_3$ is in the LS Co^{III}–HS Co^{3+} ordered state in the temperature range 110–350 K in which the electronic transport is also due to the hopping process of small polarons of holes in narrow π^*-bands [16]. Since the state being ordered means that the ratio $[Co^{III}]/[Co^{3+}]$ is fixed and thus the number of Co^{3+} ions does not increase over the range 110 K $< T <$ 350 K, the Curie constants obtained in these temperature ranges are reliable. As for $LaCo_{1-x}Ti_xO_3$, the present discussion starts from their proposal, i.e., the LS Co^{III}–HS Co^{3+} ordered state in $LaCoO_3$ for 110 K $< T <$ 350 K [16], employing the Curie constants obtained in the paramagnetic regime of figure 5 under the assumption that the number of Co^{3+} ions does not change in the paramagnetic phase, as for $LaCoO_3$.

In the 50% Co^{III} ($S = 0$) and 50% Co^{3+} ($S = 2$) ordered states of $LaCoO_3$ ($x = 0.00$), the theoretical effective magnetic moment is $\mu_{\rm eff} = 2.83\mu_{\rm B}$ which is larger in magnitude than the effective magnetic moment for the specimen with $x = 0.15$ but less than that for the specimen with $x = 0.10$. The charge neutrality in $LaCo_{1-x}Ti_xO_3$ requires divalent Co ions, i.e., Co^{II} ($S = 0.5$) or Co^{2+} ($S = 1.5$). The ratio of divalent Co ions is related to the number of Ti^{4+} ions. If a divalent Co ion is replaced with a Ti^{4+} ion, then one of the trivalent Co ions has to change into a divalent ion. Consequently, Ti^{4+} ions are substituted for Co^{III} or Co^{3+}. The ionic radius of Ti^{4+} ($r = 0.60$ Å) is nearly equal to that of Co^{3+} ($r = 0.61$ Å) but markedly larger than the radius of Co^{III} ($r = 0.52$ Å), where r is the ionic radius of Shannon and Prewitt [48]. As described before, the lattice parameters $a_{\rm H}$ and $c_{\rm H}$, and also the $c_{\rm H}/a_{\rm H}$ ratio, increase with increasing x. Antibonding electrons at Co^{2+} or Co^{II} ions certainly contribute to the lattice expansion. However, it appears that substitution of Ti^{4+} for Co^{III} must also be partly responsible for lattice expansion, like the antibonding electrons at divalent Co ions. This assertion requires further support. Based upon a fully ionic model, the shell-model calculation employed in our previous studies [32, 49–53] indicates substantial overlapping of the wave functions of Co^{3+}–O^{2-} and Co^{III}–O^{2-} pairs. However, the potential difference is only 0.4 eV in spite of such a large difference in ionic radii between Co^{3+} and Co^{III}. In oxides of strongly correlated electron systems, the covalent component in the nature of the bonding looks greater than the ionic component. Thus the substantial overlapping of the wave functions revealed in the ionic model leads to a high degree of Co 3d–O 2p hybridization in real crystals, which means that Co^{III} (t_{2g}^6) is less stable than Co^{3+} ($t_{2g}^4e_g^2$). The stabilization of lattices requires substitution of Ti^{4+} for Co^{III}.

In the specimen with $x = 0.10$, two Ti-substitution arrangements are possible. One is $LaCo^{3+}_{0.5}Co^{III}_{0.3}Co^{II}_{0.1}Ti^{4+}_{0.1}O_3$ in which Ti^{4+} ions are substituted for Co^{III} ions and 10% of the Co^{II} ions ($t_{2g}^6e_g^1$: $S = 1/2$) are transferred from Co^{III} because of the charge neutrality. The theoretical effective magnetic moment in this arrangement is $2.93\mu_{\rm B}$ which agrees well with the experimental value, i.e., $2.97\mu_{\rm B}$. Furthermore, e_g electrons in Co^{II} are itinerant, and thus could be the majority carriers which move within the lattice by hopping. This suggestion is

consistent with the negative Seebeck result. Another arrangement is $LaCo^{3+}_{0.4}Co^{III}_{0.4}Co^{2+}_{0.1}Ti^{4+}_{0.1}O_3$ in which 10% of the Co^{2+} ions ($t^5_{2g}e^2_g$: $S = 3/2$) are transferred from Co^{3+}. In this arrangement, $\mu_{eff} = 2.72\mu_B$, which is very small compared with the experimental value.

The Seebeck and magnetic measurements shown in figures 1 and 5 suggest that the electronic structure changes drastically when x increases from 0.10 to 0.15. For the specimen with $x = 0.15$, there are also two ionic arrangements possible. One is $LaCo^{3+}_{0.35}Co^{III}_{0.35}Co^{2+}_{0.15}Ti^{4+}_{0.15}O_3$ in which Ti^{4+} ions are also substituted for Co^{III} and 15% of the Co^{2+} ions are transferred from Co^{3+}. The theoretical magnetic moment in this arrangement is $2.67\mu_B$, which is comparable with the experimental result, $2.70\mu_B$. Then t_{2g} bands in HS Co ions are partially occupied, and thus the holes in these bands could be the majority carriers, as the Seebeck effect in this specimen suggests. Electrons in t_{2g} bands must be rather hard to move, because of strong electron–electron interactions. Another arrangement is $LaCo^{3+}_{0.50}Co^{III}_{0.20}Co^{II}_{0.15}Ti^{4+}_{0.15}O_3$ in which 15% of the Co^{II} ions are transferred from Co^{III}. This arrangement has the effective magnetic moment $2.99\mu_B$, which deviates greatly from the experimental moment. Despite the large number of doped Ti ions, the conductivity in the specimen with $x = 0.15$ is lower than that in the specimen with $x = 0.10$. In comparison with holes in narrow t_{2g} bands, itinerant e_g electrons are rather mobile. This must be one of the main reasons for the lower conductivity in the specimen with $x = 0.15$.

The spin state of transition metal oxides generally depends on the competition between the crystal-field-splitting energy ($10Dq$) and the exchange interaction (J), which favours HS ground states for Hund's rule couplings [54]. In $LaCoO_3$, however, $10Dq$ is just large enough to quench these interactions, stabilizing LS ground states, because of the rhombohedrally distorted perovskite structure [4]. In the $LaCo_{1-x}Ti_xO_3$ system, the rhombohedrally distorted lattice becomes less distorted with increasing x, because the c_H/a_H ratio increases. Since the idealized hexagonal ratio is $c_H/a_H = \sqrt{6}$, the specimen with $x = 0.15$ is less distorted than that with $x = 0.10$. In fact, the specimens with $x \geqslant 0.30$ become cubic perovskites [26]. The decrease in the lattice distortion leads to the decrease in $10Dq$ [19]. Zhuang *et al* predict theoretically that a decrease in $10Dq$ favours HS ground states in $LaCoO_3$ [19, 20]. This is one of the reasons for the ionic arrangement in the specimen with $x = 0.15$ and also the change in the type of the majority carrier from electrons to holes when x increases from 0.10 to 0.15.

In the case where $x = 0.05$, the arrangement in which Ti^{4+} ions are substituted for Co^{III} and 5% of the Co^{II} ions are transferred from Co^{III}, i.e., $LaCo^{3+}_{0.50}Co^{III}_{0.40}Co^{II}_{0.05}Ti^{4+}_{0.05}O_3$, has the theoretical effective magnetic moment $2.88\mu_B$, remarkably less than the experimental value, $3.19\mu_B$. So as to fit the theoretical moment to the experimental result, 7% more of the Co^{3+} ions have to be transferred from Co^{III}, i.e., the arrangement is $LaCo^{3+}_{0.57}Co^{III}_{0.33}Co^{II}_{0.05}Ti^{4+}_{0.05}O_3$. Though this is just speculative, the smallest mean ionic radius of Co and Ti ions on B sites in this ionic arrangement, i.e., 0.58 Å, in comparison with 0.59 Å and 0.60 Å for the ionic arrangements proposed for $x = 0.10$ and 0.15, supports the suggestion, because the smallest ionic radius of B-site ions results in the largest rhombohedral distortion for the specimen with $x = 0.05$.

5. Conclusion

The present study has succeeded in distinguishing the bulk conduction from the conduction across grain boundaries in the $LaCo_{1-x}Ti_xO_3$ system, using complex-plane impedance analyses. Seebeck coefficients and the magnetic properties have been measured at temperatures below 330 K. The Seebeck coefficient changes from negative to positive with x increasing from 0.10 to 0.15—i.e., the change in the type of the majority carrier from an electron to a hole is indicated. The Arrhenius relation between σT and $1/T$ for $x = 0.15$ above 190 K yields

0.24 eV for the activation energy in the bulk conduction, which is nearly equal to that for the dielectric relaxation. This implies that the hopping process of small polarons of holes dominates the transport properties for $x = 0.15$ above 190 K.

The temperature dependence of the magnetic susceptibilities indicates that the number of HS Co^{3+} ions decreases with increasing x. The expansion of the lattice parameters in $LaCo_{1-x}Ti_xO_3$, a_H and c_H, with increasing x requires the replacement of LS Co^{III} with Ti^{4+}. Furthermore, substitution of Ti for Co^{III} relaxes the rhombohedral distortion in the $LaCo_{1-x}Ti_xO_3$ system, and thus leads to a decrease in magnitude for the crystal-field-splitting energy $10Dq$. The decease in $10Dq$ favours HS ground states. The effective magnetic moments estimated from the Curie constants in the relations between χ^{-1} and T suggest that itinerant e_g electrons on Co^{II} could be the majority carriers in the specimen with $x = 0.10$, and the holes in the partially occupied t_{2g} bands could be the majority carriers for $x = 0.15$. These majority carriers move in the lattices by hopping.

Acknowledgments

The authors are very grateful to J Noro for the chemical analyses, and are also indebted to F Munakata and W H Jung for their useful advice and discussions of this project. This project was supported by Takahashi Industrial and Economic Research Foundation. The dc conductivity and Seebeck coefficients were measured at the Instrumental Analysis Centre at Yokohama National University. The SQUID magnetometer in the Ecotechnology System Laboratory, Yokohama National University, was used.

References

[1] Heikes R R, Miller R C and Mazelsky R 1964 *Physica* **30** 1600
[2] Naiman C S, Gilmore R, DiBartolo B, Linz A and Santoro R 1965 *J. Appl. Phys.* **36** 1044
[3] Jonker G H 1966 *J. Appl. Phys.* **37** 1424
[4] Raccah P M and Goodenough J B 1967 *Phys. Rev.* **155** 932
[5] Bhide V G, Rajoria D S, Rao G R and Rao C N R 1972 *Phys. Rev.* B **6** 1021
[6] Thornton G, Tofield B C and Williams D E 1982 *Solid State Commun.* **44** 1213
[7] Asai K, Gehring P, Chou H and Shirane G 1989 *Phys. Rev.* B **40** 10 982
[8] Itoh M and Natori I 1995 *J. Magn. Magn. Mater.* **140–144** 2145
[9] Yamaguchi S, Okimoto Y, Taniguchi H and Tokura Y 1996 *Phys. Rev.* B **53** R2926
[10] Asai K, Yokokura O, Nishimori N, Chou H, Tranquada J M, Shirane G, Higuchi S, Okajima Y and Kohn K 1994 *Phys. Rev.* B **50** 3025
[11] Chainani A, Mathew M and Sarma D D 1992 *Phys. Rev.* B **46** 9976
[12] Chainani A, Mathew M and Sarma D D 1993 *Phys. Rev.* B **47** 15 397
[13] Abbate M, Fuggle J C, Fujimori A, Tjeng L H, Chen C T, Potze R, Sawatzky G A, Eisaki H and Uchida S 1993 *Phys. Rev.* B **47** 16 124
[14] Abbate M, Potze R, Sawatzky G A and Fujimori A 1994 *Phys. Rev.* B **49** 7210
[15] Barman S R and Sarma D D 1994 *Phys. Rev.* B **49** 13 979
[16] Señarís-Rodríguez M A and Goodenough J B 1995 *J. Solid State Chem.* **116** 224
[17] Korotin M A, Ezhov S Yu, Solovyev I V, Anisimov V I, Khomskii D I and Sawatzky G A 1996 *Phys. Rev.* B **54** 5309
[18] Mizokawa T and Fujimori A 1996 *Phys. Rev.* B **54** 5368
[19] Zhuang M, Zhang W and Ming N 1998 *Phys. Rev.* B **57** 10 705
[20] Zhuang M, Zhang W, Hu C and Ming N 1998 *Phys. Rev.* B **57** 10 710
[21] Iguchi E, Ueda K and Jung W H 1996 *Phys. Rev.* B **54** 17 431
[22] Emin D and Holstein T 1969 *Ann. Phys., NY* **53** 439
[23] Lang I G and Firsov Yu A 1968 *Zh. Eksp. Teor. Fiz.* **54** 826
[24] Austin I G and Mott N F 1969 *Adv. Phys.* **18** 41
[25] Iguchi E, Ueda K and Nakatsugawa H 1998 *J. Phys.: Condens. Matter* **10** 8999

[26] Bahadur D and Parkash Om 1983 *J. Solid State Chem.* **46** 197
[27] Iguchi E, Kubota N, Nakamori T, Yamamoto N and Lee K J 1991 *Phys. Rev.* B **43** 8646
[28] Iguchi E and Akashi K 1992 *J. Phys. Soc. Japan* **61** 3385
[29] Lee K J, Iguchi A and Iguchi E 1993 *J. Phys. Chem. Solids* **54** 975
[30] Iguchi E and Jung W H 1994 *J. Phys. Soc. Japan* **63** 3078
[31] Jung W H and Iguchi E 1995 *J. Phys.: Condens. Matter* **7** 1215
[32] Iguchi E, Hashimoto T and Yokoyama S 1996 *J. Phys. Soc. Japan* **65** 221
[33] Jung W H and Iguchi E 1996 *Phil. Mag.* B **73** 873
[34] Iguchi E, Nakamura N and Aoki A 1997 *J. Phys. Chem. Solids* **58** 755
[35] Jung W H, Nakatsugawa H and Iguchi E 1997 *J. Solid State Chem.* **133** 466
[36] Iguchi E, Nakamura N and Aoki A 1998 *Phil. Mag.* B **78** 65
[37] Jung W H and Iguchi E 1998 *J. Phys. D: Appl. Phys.* **31** 794
[38] Iguchi E, Nakatsugawa H and Futakuchi K 1998 *J. Solid State Chem.* **139** 176
[39] MacDonald J R 1974 *J. Chem. Phys.* **61** 3977
[40] MacDonald J R 1976 *Superionic Conductors* ed S D Mahan and W L Roth (New York: Plenum) p 81
[41] Bauerle J E 1969 *J. Phys. Chem. Solids* **30** 2657
[42] Franklin A D 1975 *J. Am. Ceram. Soc.* **58** 465
[43] Kurusu K, Takami H and Shintomi K 1989 *Analyst* **114** 1341
[44] Dominik L A K and MacCrone R K 1967 *Phys. Rev.* **163** 756
[45] Frölich H 1958 *Theory of Dielectrics* (Oxford: Clarendon) p 70
[46] Emin D 1974 *Phys. Rev. Lett.* **32** 303
[47] Emin D 1982 *Phys. Today* **35** 34
[48] Shannon R D and Prewitt C T 1969 *Acta Crystallogr.* B **25** 925
[49] Aizawa K, Iguchi E and Tilley R J D 1984 *Proc. R. Soc.* A **394** 299
[50] Iguchi E, Tamenori A and Kubota N 1992 *Phys. Rev.* B **45** 697
[51] Iguchi E and Nakatsugawa H 1995 *Phys. Rev.* B **51** 10 956
[52] Nakatsugawa H and Iguchi E 1997 *Phys. Rev.* B **55** 2157
[53] Nakatsugawa H and Iguchi E 1997 *Phys. Rev.* B **56** 12 931
[54] Rao C N R, Parkash Om and Ganguly P 1975 *J. Solid State Chem.* **15** 186